Membrane Topology of the Melibiose Permease of *Escherichia coli* Studied by *melB*−*phoA* Fusion Analysis†

Thierry Pourcher,‡ Eitan Bibi,§,|| H. Ronald Kaback,§ and Gérard Leblanc*,‡

Laboratoire J. Maetz, Département de Biologie Cellulaire et Moléculaire/CEA, O6230 Villefranche sur Mer, France, and Howard Hughes Medical Institute, Departments of Physiology and Microbiology & Molecular Genetics, University of California, Los Angeles, California 90024-1662

Received November 20, 1995; Revised Manuscript Received February 2, 1996⊗

ABSTRACT: In order to study the secondary structure of the melibiose permease of *Escherichia coli*, 57 *melB*−*phoA* gene fusions were constructed and assayed for alkaline phosphatase activity. In general agreement with a previously suggested secondary structure model of melibiose permease [Botfield, M. C., Naguchi, K., Tsuchiya, T., & Wilson, T. H. (1992) *J. Biol. Chem. 267*, 1818], clusters of fusions exhibiting low and high phosphatase activity fusions alternate along the primary sequence. Fusions with high activity generally cluster at residues predicted to be in the periplasmic half of transmembrane domains or in periplasmic loops, while fusions with low activity cluster at residues predicted to be in the cytoplasmic half of transmembrane domains or in cytoplasmic loops. Taken together, the findings strongly support the contention that melibiose permease contains 12 transmembrane domains that traverse the membrane in zigzag fashion connected by hydrophilic loops that are exposed alternatively on the periplasmic or cytoplasmic surfaces of the membrane with the N and C termini on the cytoplasmic face of the membrane. Moreover, on the basis of the finding that the cytoplasmic half of an out-going segment is sufficient for alkaline phosphatase export to the periplasm while the periplasmic half of an in-going segment prevents it [Calamia, T., & Manoil, C. (1990) *Proc. Natl. Acad. Sci. U.S.A. 87*, 4937], the activity profile of the melibiose permease−alkaline phosphatase fusions is consistent with the predicted topology of seven of 12 transmembrane segments. However, five transmembrane domains require adjustment, and as a consequence, the size of the central cytoplasmic loop is reduced and a significant number of charged residues are shifted from a hydrophilic to a hydrophobic domain in this region of the transporter.

The melibiose (Mel) permease of *Escherichia coli* is an integral membrane protein that catalyzes accumulation of α-D-galactopyranosides by cation-solute symport or co-transport (Lopilato et al., 1978). Depending on the ionic environment and/or the configuration of the sugar substrate, Mel permease utilizes Na^+, H^+, or Li^+ as the coupling ion [reviewed by Pourcher et al. (1990a)]. The cation recognition properties of Mel permease have been analyzed by using site-directed mutagenesis (Pourcher et al., 1993; Wilson & Wilson, 1992, 1994; Zani et al., 1993, 1994) or by fusing complementary domains of homologous Mel permease molecules to produce chimeric symporters (Hama & Wilson, 1993). The results suggest that residues in the N-terminal hydrophobic domains of the transporter are involved in cation recognition. It has also been hypothesized (Pourcher et al., 1993) that several acidic residues in neighboring helices may act as a network for coordination of the coupling cation. However, in order to define the mechanism of action of Mel permease, structural information is required.

Examination of the sequence of the *melB* gene which encodes Mel permease led to the finding that the transporter consists of 469 amino acid residues (52 029 Da), 70% of which are apolar (Yazyu et al., 1984). Recent determination of the N-terminal sequence of the purified protein essentially confirms this prediction but also demonstrates that three additional residues precede the predicted N-terminal residue and that the mature permease lacks a Met residue at the N terminus (Pourcher et al., 1995). On the basis of hydropathy profiling of the primary amino acid sequence of Mel permease and additional predictive methods (Pourcher et al., 1990; Botfield et al., 1992), the secondary structure of *mel* permease was postulated to contain 12 transmembrane domains in α-helical conformation that traverse the membrane in zigzag fashion connected by hydrophilic loops with the N and C termini on the cytoplasmic surface of the membrane (Figure 1).

A gene-fusion approach pioneered by Manoil and Beckwith (1986) utilizing the *phoA* gene which encodes alkaline phosphatase has been used to evaluate the topological predictions for several bacterial transporters (Gött & Boos, 1988; Calamia & Manoil, 1990; Lloyd & Kadner, 1990; Boyd et al., 1993; Ujwal et al., 1995). Alkaline phosphatase is synthesized as an inactive precursor in the cytoplasm of *E. coli* with a short signal sequence that directs its secretion into the periplasmic space, where it dimerizes to form active

† This work was supported in part by the Centre National de la Recherche Scientifique (URA 1855) and by grants from NATO (G.L. and H.R.K.) and from Human Frontier Science Organization (G.L.).

* Author to whom correspondence should be addressed at Laboratoire J. Maetz/CEA, BP 68, 06230 Villefranche sur Mer, France. FAX: (33) 93 76 60 17. E-mail: Leblanc@ccrv.obs-vlfr.fr.

‡ Laboratoire J. Maetz.

§ Howard Hughes Medical Institute.

|| Present adress: Department of Biochemistry, Weizmann Institute of Science, Rehovot, 76100, Israel.

⊗ Abstract published in *Advance ACS Abstracts,* March 15, 1996.

0006-2960/96/0435-4161$12.00/0

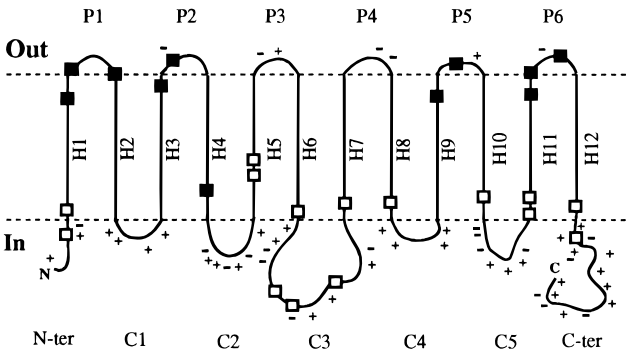

FIGURE 1: Schematic representation of the secondary structure model of Mel permease based on hydropathy analysis, secondary structure predictions, and analysis of a limited number of *melB*−*phoA* fusions (□, ■) obtained by a *TnphoA* insertion strategy (Botfield et al., 1992). Open and filled squares correspond to fusions with low (<15 units) or high alkaline phosphatase activity (>25 units), respectively. H1−H12, membrane-spanning segments; P1−P6, periplasmic loops; C1−C5, cytoplasmic loops.

enzyme. If the signal sequence is deleted, then the enzyme remains in the cytoplasm in an inactive form. When alkaline phosphatase devoid of the signal sequence is fused to the C termini of fragments of a cytoplasmic membrane protein, enzyme activity reflects the ability of the N-terminal portions of the chimeric polypeptides to translocate alkaline phosphatase to the outer surface of the membrane.

In addition, it has been shown with the lactose permease of *E. coli* that the cytoplasmic-half of an out-going segment promotes alkaline phosphatase translocation to the periplasmic surface of the membrane while the periplasmic-half of an in-going segment prevents it. Thus, the alkaline phosphatase activity of fusions engineered at every third amino acid residue in putative helices III and V (Calamia & Manoil, 1990), at alternative residues in helices VII and IX (Ujwal et al., 1995), and at every residue in helices IX and X (M. L. Ujwal, E. Bibi, C. Manoil, and H. R. Kaback, unpublished information) increases sharply as the fusion junction proceeds through three residues moving toward the C terminus.

Botfield et al. (1992) utilized *melB*−*phoA* fusions to test the predicted secondary structure of Mel permease, and the fusion junctions obtained with 28 *TNphoA* transposon insertions, as well as their alkaline phosphatase activity, are indicated in Figure 1. The results conform generally with the proposal that Mel permease traverses the membrane several times. However, the random character of the transposon insertion technique used to generate the chimeras does not allow precise definition of several regions in the permease. The absence of low-activity fusions in the N-terminal portion of Mel permease (helices I−IV) prevents clear assignment of the cytoplasmic loops in this region. In addition, no high-activity fusions were described that allow assignment of periplasmic loops in the central region of the permease (helices IV−VIII).

In this paper, engineered *melB*−*phoA* fusions are used to examine the topology of Mel permease more precisely. The properties of fusions constructed at 3−5-residue intervals in each predicted transmembrane domain and in relatively ill-defined loops are described. The analysis provides confirmation of the topological predictions of the 12-transmembrane domain model but also suggests several important modifications.

MATERIALS AND METHODS

Materials. Most of the dideoxyoligonucleotides used in this study were synthesized on an Applied Biosystems 391 DNA synthesizer by Kerstin Stemple. Additional dideoxyoligonucleotides were obtained from Eurogentec (Belgium). Restriction endonucleases, Klenow DNA polymerase, T4 polynucleotide kinase, and T4 DNA ligase were obtained from Boehringer Mannheim and New England Biolabs. Sequenase and sequenase reaction kits, Vent polymerase, and associated polymerase chain reaction (PCR) reagents were from United States Biochemicals. Isopropyl 1-thio-β-D-galactopyranoside (IPTG), *p*-nitrophenyl phosphate (NPP), 5-bromo-4-chloro-3-indolyl phosphate, *p*-toluidine salts (XP), and *E. coli* alkaline phosphatase (EC 3.1.3.1, type III) were from Sigma. Prestained molecular weight markers were from Bio-Rad. Mouse antibacterial alkaline phosphatase was obtained from Caltag Laboratories Inc. (San Francico, CA). Polyvinylidene difluoride (PVDF) transfer membranes were from NEN (Dupont). Enhanced chemiluminescence (ECL) Western blotting detection kits were purchased from Amersham. All other reagents were reagent grade and obtained from commercial sources.

Bacterial Strains. E. coli CC118 (*ara* D139 Δ[*ara leu*] 7697 Δ*lac* X74 Δ*phoA* 20 *gal*E *gal*K *thi rps*E *rpo*B *arg*E-[am] *rec*A1) (Calamia & Manoil, 1990) transformed with plasmids encoding given *melB*−*phoA* fusions was used to measure the alkaline phosphatase activity of the chimeras.

Construction of Plasmids Encoding melB−*phoA Fusions.* A two-step stategy was used to construct the *melB*−*phoA* chimeric genes [cf. Ujwal et al. (1995)]. First, DNA fragments encoding increasing lengths of *melB* with a *Bam*HI restriction site at the 5′ end of the reading frame and an *Nhe*I site at the 3′ end were generated by PCR amplification from a *melB* template in plasmid pK60. The *Bam*HI−*Nhe*I restriction fragments were then inserted in place of the *lacY* gene in pT7-5(*lacY*−*phoA*) (Ujwal et al., 1995).

Plasmid pK60 is a recombinant pKK 223-3 (Pharmacia) plasmid derived from pK50 (Zani et al., 1994) which is deleted of the first 516 base pairs of *melA* and with the *melB* gene under the control of the *tac* promoter. The *melB* sequence is flanked by unique *Eco*RI or *Hin*dIII sites at the 5′ and 3′ ends, respectively, and contains unique *Kpn*I and *Eco*RV sites in the DNA encoding the cytoplasmic loops connecting membrane-spanning segments H4−H5 and H10−H11, respectively. Unique restriction sites were created in the remaining cytoplasmic loops. A *Pst*I *site* and a *Bst*EII site were created in the DNA encoding the cytoplasmic loops between H6 and H7 and between H8 and H9 using the primers 5′-AAT CAA CCG **TCT GCA G**AA GGA AGC C-3′ and 5′-GCT AAC CT**G GTG ACC** TTA GTA TTC TTC C-3′, respectively. An undesired *Bam*HI site in the DNA encoding the loop between H2 and H3 was converted into a *Sty*I site using the mutagenic primer 5′-G TTC AAA **CCA TGG** ATT CTG ATC GGT ACG-3′. For convenience, a *Bam*HI site and a nearby *Sty*I site upstream of the *tac* promoter were removed by linearizing pK50 with *Sty*I, followed by partial digestion with *Bam*HI, Klenow end-filling, and ligation of blunt ends. All modifications of the reading sequence of *melB* were designed so as to result in silent mutations.

Plasmid pT7-5(*lacY*−*phoA*) plasmid carries the cassette *lacY* gene (EMBL X-56095) under the control of both the

T7 and *lacZ* promoters fused in-frame with a *phoA* gene devoid of the signal sequence (Ujwal et al., 1995). The *lacY* coding sequence is preceeded by a *Bam*HI site and followed by an *Nhe*I site, 48 base pairs, and a 5′-truncated *phoA* coding sequence that starts with a codon corresponding to the sixth amino acid of mature alkaline phosphatase. The 48 base-pair linker between the *lacY* and *phoA* sequences and the *phoA* sequence are identical to those in *TnphoA*, thereby permitting comparison of the relative activities of the fusions studied here with those described by Botfield et al. (1992). Plasmid pT7-5(*lacY*−*phoA*) was digested with with *Bam*HI and *Nhe*I in order to remove the *lacY*−*phoA* sequences (linearized pT7-5) and used for insertion of the *melB*−*phoA* chimeras.

PCR amplification of *melB*−*phoA* fragments from pK60 was performed by using a common 32-mer sense primer (5′-TTT A**GC ATC C***AT GAC TAC AAA ACT CAG TTA*-3′) containing a *Bam*HI site (bold) and the first 20 nucleotides of *melB* (italics) and a variable antisense primer (5′-ATT TAA **GCT AGC** $[X]_n$). The latter carries an *Nhe*I site (bold) followed by a 13−18-nucleotides stretch $[(X)_n]$ which corresponds to four to six codons terminating the *melB* sequence to be fused. The DNA fragments were restricted with *Bam*HI and *Nhe*I, phosphorylated, and ligated into linearized pT7-5. With fusions downstream of the *Pst*I site in the *melB* sequence, PCR fragments were digested at a convenient unique restriction site in the *melB* sequence (*Kpn*I, *Pst*I, or *Bst*EII) and *Nhe*I. Purified *Kpn*I-, *Pst*I-, or *Bst*EII−*Nhe*I fragments were used to extend the length of the *melB* sequence in previously constructed fusion plasmids. The nucleotide sequences of all ligated DNA fragments as well as the 5′ and 3′ ends were systematically verified by dideoxynucleotide sequencing.

Alkaline Phosphatase Activity. The alkaline phosphatase activity of *E. coli* CC118 expressing the chimeras was measured as described by Michaelis et al. (1983). Briefly, cells were transformed with given plasmids and grown for 2 h in LB medium in the presence of 10 mM IPTG and ampicillin (100 μg/mL). Cells were collected by centrifugation, washed twice with 1.0 M Tris-HCl (pH 8.0), and resuspended in the same medium to give an OD_{600} of about 1. Activity was immediately assayed in the presence of *p*-nitrophenyl phosphate (0.66 mg/mL) at 37 °C and expressed in units of $OD_{420} \times 1000/OD_{600} \times$ time. Each value given is the mean value of duplicate determinations corrected for background activity measured in untransformed host cells (ca. 6−8 units/OD_{600}). Variations in the activity of a given fusion measured in different clones was less than 10%.

Detection of the Mel Permease−Alkaline Phosphatase Fusion Proteins. E. coli CC118 expressing the fusion proteins were grown and treated as described for alkaline phosphatase measurements. Aliquots were subjected to sodium dodecyl sulfate ($NaDodSO_4$)−polyacrylamide gel electrophoresis using 12% polyacrylamide (Pourcher et al., 1990b). Proteins were electroblotted on PVDF membranes which were then incubated with mouse antibacterial alkaline phosphatase monoclonal antibodies (1/10 000 dilution). Following incubation with horseradish peroxidase-coupled, anti-mouse antibodies (1/2000 dilution), the immunoreactive polypeptides were detected using the Amersham ECL Western blotting system. Where indicated, experiments were carried out on membrane vesicles prepared by an osmotic chock procedure (Kaback, 1971).

Protein. Protein was measured as described (Lowry et al., 1951) using bovine serum albumin as standard.

RESULTS

Construction of melB−phoA Fusions. Fifty-seven *melB*−*phoA* chimeras encoding N-terminal Mel permease fragments of varying length fused to alkaline phosphatase at specified sites were constructed as described in Materials and Methods. Individual fusions are identified by the amino acid in Mel permease immediately preceding the junction site and its residue number (Table 1, column 1). The locations of junction sites in putative membrane-spanning segments (H), periplasmic loops (P), cytoplasmic loops (C), or in the C-terminal tail (CT) are also given in Table 1 (column 2). With the exceptions of L99 and L426, the fusion junctions in all of the chimeras described differ from those of Botfield et al. (1992).

Alkaline Phosphatase Activity. The alkaline phosphatase activity of each Mel permease−alkaline phosphatase fusion expressed in *E. coli* CC118 *(*Δ*phoA*) was measured after 2 h of induction in the presence of IPTG (Table 1). Activity varies over a broad range, from no significant activity to 137 ± 10 units (Table 1, column 3). The position and activity of each fusion relative to the 12-transmembrane domain model of Mel permease proposed by Botfield et al. (1992) are indicated in Figure 2. Four of the fusions were constructed with junctions in putative periplasmic loops, four are in proposed cytoplasmic loops, two are in the C-terminal tail, and the remainder are in putative transmembrane domains. Cells expressing fusions with the junctions in predicted periplasmic loops [G45 in P1, V111 in P2, G176 in P3, and G263 in P4] exhibit high alkaline phosphatase activities ranging from 56 to 92, as indicated by the filled circles. In contrast, fusions with junctions in postulated cytoplasmic loops (G74 in C1, V145 in C2, E203 in C3, or Y358 in C5), do not exhibit activity above that of untransformed *E. coli* CC118, as indicated by the open circles. Cells expressing the two fusions in the C-terminal tail (F430 and G437) also exhibit little or no activity, a finding consistent with immunological evidence demonstrating that the C terminus of Mel permease is accessible exclusively from the cytoplasmic surface of the membrane (Botfield & Wilson, 1989). The results provide additional support for the topological predictions of the 12-transmembrane domain motif (Botfield et al., 1992; Pourcher et al., 1990).

The remaining 47 fusions were constructed with junctions in putative membrane-spanning segments with a minimum of three fusions in each hydrophobic domain (Figure 2, Table 1). A transition from high to low activity is observed in every putative membrane-spanning segment except H2 and H4, where all of the chimeras exhibit little or no activity. The transition occurs abruptly over a short stretch of amino acids in H1, H3, H9, H11, or H12. In contrast, the transition appears to be more progressive in H5 to H8 and H10 where a chimera with intermediate activity is interposed between the low- and high-activity fusions (cross-hatched circles).

In four membrane-spanning segments (H3, H8, H9, and H12), the transition from low to high activity is observed at the approximate middle of the postulated transmembrane domain (Figure 2; Table 1). In the other chimeras, the transition is displaced from the middle of the transmembrane domain toward either the periplasmic (H2, H4, H5, H10, and

Table 1: Location and PhoA Activity of MelB−PhoA Hybrid Proteins

N-terminal domain			central domain			C-terminal domain		
fusion	location	PhoA activity[b]	fusion	location	PhoA activity[b]	fusion	location	PhoA activity[b]
V25	H1	0	V145	C2	0	I297	H9	0
M30	H1	112	T159	H5	9	L305	H9	0
G38	H1	20	T163	H5	34	G311	H9	71
G45	P1	83	N168	H5	98	I329	H10	64
V50	H2	7	G176	PL3	80	N335	H10	34
W54	H2	0	F182	H6	106	F341	H10	0
A56	H2	0	A188	H6	94	Y358	C5	0
P60	H2	2	V192	H6	73	A381	H11	0
W64	H2	0	I196	H6	34	A388	H11	14
V66	H2	0	E203	C3	6	G395	H11	72
G74	C1	0	A240	H7	3	M410	H12	125
G83	H3	0	N244	H7	47	I415	H12	76
V89	H3	105	I249	H7	112	L420	H12	14
A97	H3	137	G252	H7	106	L426	H12	18
L99	H3	114	F258	H7	115	F430	CT	10
V111	P2	56	G263	P4	92	G437	CT	0
I114	H4	20	P269	H8	72			
G117	H4	4	S273	H8	87			
T121	H4	4	A277	H8	26			
T133	H4	0	T282	H8	1			

[a] All listed MelB−PhoA fusion proteins are encoded by PT7-5 recombinant plasmids constructed *in vitro* as described under Materials and Methods. Each fusion (columns 1, 4, and 7) is identified by the last residue of the MelB domain in the MelB−PhoA hybrid protein. The one-letter amino acid codes and numbers indicate the position of the identifying residue in the revised wild-type Mel permease sequence (Pourcher et al., 1995). Columns 2, 5, and 8 indicate the locations of the identifying residues in putative membrane-spanning segments (H1−12), periplasmic loops (P1−P6), cytoplasmic loops (C1−C5), or cytoplasmic tail (CT) of Mel permease (Botfield et al., 1992). PhoA activity was measured on permeabilized *E. coli* CC118 cells transformed with each plasmid and previously induced for 2 h in the presence of IPTG (columns 3, 6, and 9). Rate of *p*-nitrophenyl phosphate hydrolysis was measured at OD_{420} (Michaelis et al., 1983), normalized for sample protein concentration (OD_{600}), and corrected for the background activity measured in control CC118 cells (usually 5 units OD_{420}/OD_{600}). The difference in PhoA activity measured in different clones expressing the same fusion protein was less than 15%. [b] In units/OD_{600}.

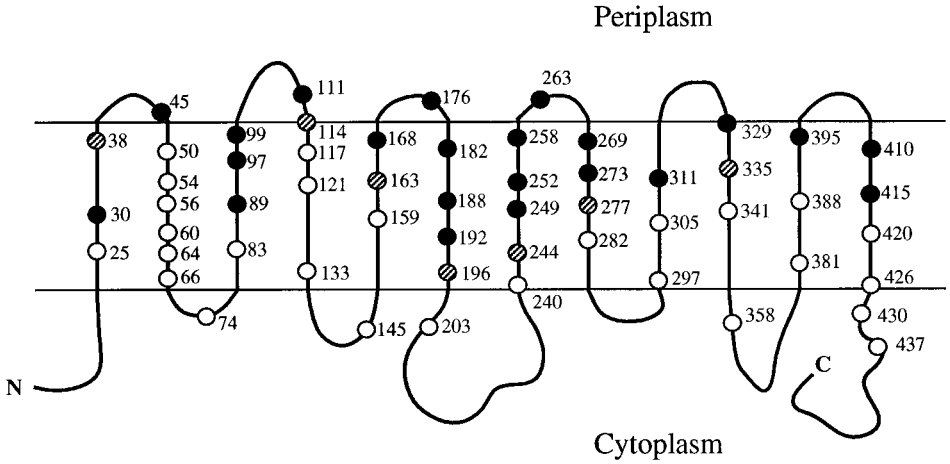

FIGURE 2: Distribution and activity of 57 site-directed *melB−phoA* fusions with junction points in membrane-spanning segments or periplasmic or cytoplasmic loops of Mel permease. The model shown is from Botfield et al. (1992). *E. coli* CC118 was transformed with given plasmids and grown for 2 h in the presence of 10 mM IPTG. Alkaline phosphatase activity was measured in permeabilized cells (see Materials and Methods). Fusions are indicated by the position of the last residue of the fused Mel permease sequence and are numbered sequentially from the N terminus according to the revised primary amino acid sequence of Mel permease (Pourcher et al., 1995). Open, cross-hatched, and filled circles represent low (<20 units), intermediate (20−50 units), or high (>50 units) alkaline phosphatase activity, respectively.

H11) or the cytoplasmic (H1, H6, and H7) end of the domain. In particular, the transition is clearly off-center in H2, H4, H6, and H7. Thus, all fusions in H6 and all but one fusion at the presumed cytoplasmic end of H7 (N244) display significant activity. At the other extreme, all of the fusions in H2 and H4 exhibit little or no activity. Incidentally, the lack of activity of the fusions in H2 may be due to Arg52 in the periplasmic half of this domain which may be ion-paired in mature Mel permease. Thus, Calamia and Manoil (1992) have reported that Arg302 (helix IX), which is normally ion-paired with Glu325 in Lac permease (Jung et al., 1993; He et al., 1995b), impairs the ability of transmembrane domain X to act as a signal sequence for alkaline phosphatase export because of its charged nature. However, it is unlikely that Arg52 in Mel permease behaves in a similar fashion for two reasons. First, the activity of fusion V50, which does not carry Arg52, is already very low. Second, the activity of fusion W54 remains low even when Arg52 is replaced with Ala (data not shown).

The activity profile of the chimeras analyzed in this study and those described by Botfield et al. (1992), relative to the predicted secondary structure model of Mel permease, is shown in Figure 3A. Clearly, both sets of data agree with the findings of Botfied et al. (1992) and demonstrate that

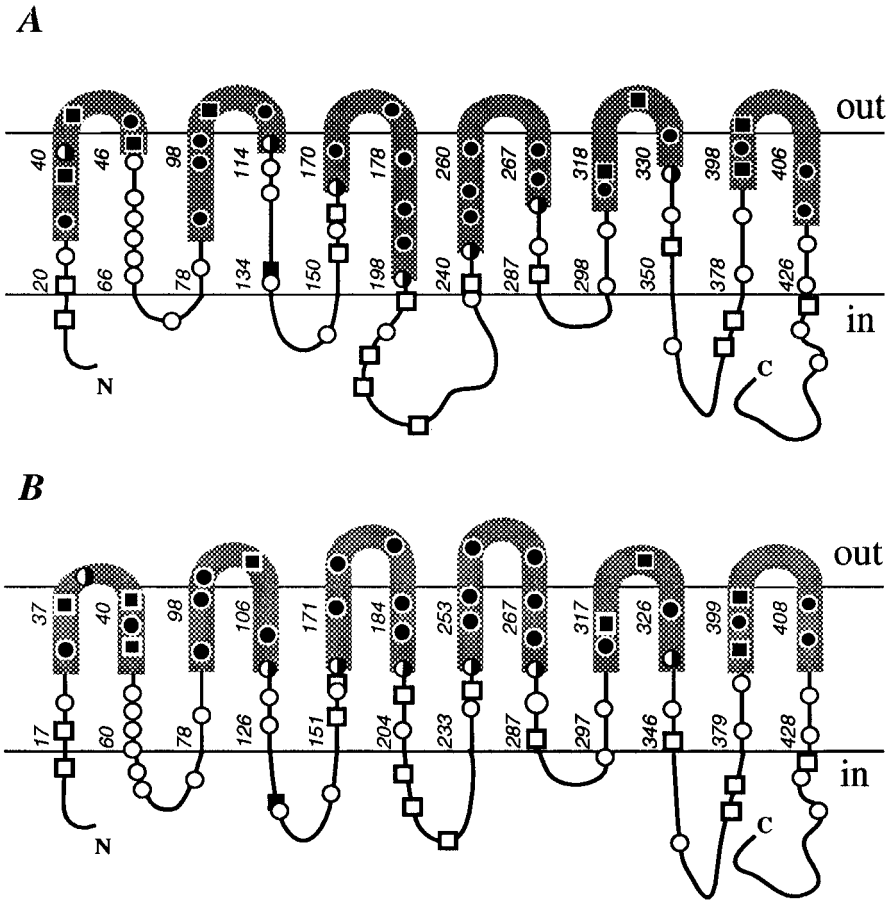

FIGURE 3: Revision of the secondary structure model of Mel permease. The position and alkaline phosphatase activity of the Mel permease−alkaline phosphatase fusions described here and in Botfield et al. (1992) are superimposed on the previous secondary structure model (Botfield et al., 1992) (A) or on the revised model (B). (○, ◑, ●) Data from Figure 2, indicating fusions with low, intermediate, or high PhoA activity, respectively. (□, ■) Data from Botfield et al. (1992), indicating fusions with low or high alkaline phosphatase activity. Revision of Mel permease secondary structure model is based on the assumption that the transition from high to low alkaline activity occurs at the approximate middle of each transmembrane domain. Residues ending each membrane-spanning segment are numbered according to the revised primary amino acid sequence of Mel permease (Pourcher et al., 1995).

clusters of high-activity fusions alternate systematically with clusters of low-activity fusions. Moreover, fusions with high activity generally cluster in the outer half of the putative transmembrane domains and in periplasmic loops, while low-activity fusions cluster in the inner half of the transmembrane domains and in cytoplasmic loops. Finally, with the exception of G38 (Botfield et al., 1992), fusions with intermediate activity are found between the high- and low-activity clusters.

Relationship between Activity and Expression of the Chimeras. Expression of the Mel permease−alkaline phophatase chimeras was measured by immunoblot analysis of cells or membranes using an antibody against the alkaline phosphatase moiety. Experiments were carried out on *E. coli* CC118 treated under conditions identical to those used to measure alkaline phosphatase activity. Representative examples are shown in Figure 4. An immunoblot of the total cell extract from cells expressing three highly active chimeras (G45, S273, and M410; Table 1) indicates extensive degradation of the fusion proteins (left gel). In all three cases, the antibody reacts strongly with a major breakdown product that exhibits an M_r comparable to that of mature alkaline phosphatase (filled diamonds). The full-length products are observed more readily in immunoblots of the cytoplasmic membranes and generally exhibit lower M_r values than theoretical (right gel, empty triangles). For unknown reasons, G45 gives little full-length chimera. This is most likely due

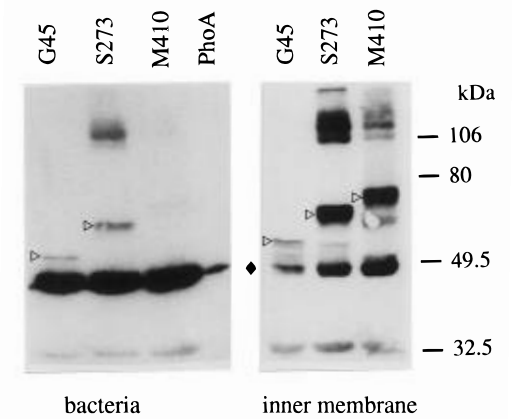

FIGURE 4: Immunoblot analysis of fusions G45, S273, and M410 conferring high alkaline phosphatase activity. *E. coli* CC118 cells, expressing each fusion protein, were grown in LB and induced for 2 h in the presence of 10 mM IPTG. Total cell protein (60 μg) or protein from purified inner membranes (40 μg) was subjected to 12% $NaDodSO_4$−polyacrylamide gel electrophoresis and electroblotted. Blots were incubated first with mouse antibacterial alkaline phosphatase monoclonal antibodies, then with horseradish peroxydase anti-mouse antibodies, and finally with ECL chemiluminescent reagent (△): Full-length chimera; (◆): major breakdown product remaining associated with the membrane fraction.

to high instability of this particular chimera as the associated alkaline phosphatase-like breakdown product is high. In addition to proteolysis products and full-length chimeras,

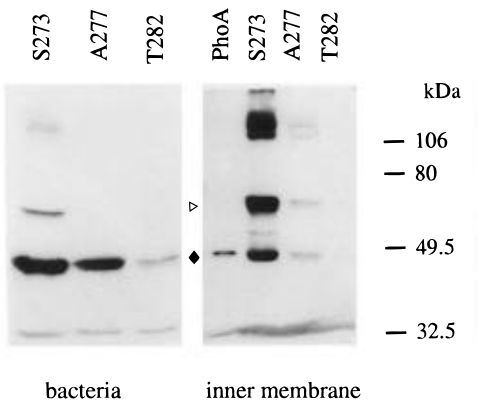

FIGURE 5: Immunoblot analysis of three Mel permease−alkaline phosphatase fusions confering high (S273), intermediate (A277), or low (T282) alkaline phosphatase activity. *E. coli* CC118 expressing given fusion proteins were grown in LB and induced for 2 h in the presence of IPTG (10 mM). Total cell protein (60 μg) or protein from purified inner membranes (40 μg) was subjected to 12% $NaDodSO_4$−polyacrylamide gel electrophoresis, electroblotted, and processed for immunodetection with mouse antibacterial alkaline phosphatase monoclonal antibodies. Left or right gel corresponds to cell or inner membrane proteins, respectively. The lane labeled PhoA corresponds to pure bacterial alkaline phosphatase (0.02 μg). (△): Full-length chimera; (◆): major breakdown product.

dimers are also observed with fusions S273 and M410 (upper intense bands). Proteolysis of fusion proteins has been observed frequently with several other transporters (Gött & Boos, 1988; Calamia & Manoil, 1990; Lloyd & Kadner, 1990; Ujwal et al., 1995), and, in addition, the alkaline phosphatase activity exhibited by the chimeras is correlated with the sum of the activities of the intact chimera and the mature alkaline phosphatase released rather than with the full-length chimera itself.

In several postulated transmembrane domains (H5, H7, H8, and H10), the transition from high to low activity is interceded by a chimera that exhibits intermediate activity. In these intermediate-activity fusions, immunoblot analysis indicates that a decrease in the level of expression of the full-length chimeras and the degradation products is correlated with the decreased activity. Representative examples are shown in Figure 5. The activity of fusions S273, A277, and T282 in H8 is 87, 26, and 1 OD_{400} units/OD_{600}, respectively (Table 1). Immunoblot analysis of total cell proteins from these clones shows that the full-length fusion protein is observed only in cells expressing fusion S273 and that the proportion of mature alkaline phosphatase released decreases such that S273 > A277 ≫ T282 (left gel). The difference in the level of expression of the three chimeras and their degradation products is also observed with purified membranes (right gel). It is striking that neither the full-length protein nor the immunoreactive degradation product of the low-activity fusion T282 is observed. In general, full-length chimeras and degradation products are seldom detected with low-activity fusions regardless of their location (not shown). This observation is consistent with previous observations (Gött & Boos, 1988; Lloyd & Kadner, 1990; Ujwal et al., 1995) demonstrating that fusions which do not lead to export of the alkaline phosphatase moiety across the membrane are particularly unstable and proteolyzed rapidly.

DISCUSSION

Characterization of a set of 57 engineered Mel permease−alkaline phosphatase fusion proteins described here provides important additional information regarding the topology of Mel permease and, in particular, of its transmembrane domains. On one level, the data support the proposal that Mel permease contains 12 membrane-spanning domains (Botfield et al., 1992). Moreover, on the basis of the finding that the cytoplasmic halves of out-going segments are needed to translocate alkaline phosphatase to the periplasmic surface of the membrane while the periplasmic halves of in-going segments prevent it (Calamia & Manoil, 1990), the pattern of activity displayed by the chimeras supports the predicted composition of seven of 12 membrane-spanning segments. On another level, however, five of the putative membrane-spanning segments (H2, H4, H6, H7, and H10) require significant alteration. As a consequence, the size of the central cytoplasmic loop is reduced, and charged residues previously thought to be located exclusively in N-terminal hydrophobic domains are also present in the central hydrophobic domains of the permease as well.

Judging from the level of alkaline phosphatase activity of cells expressing the 57 chimeras, three classes of fusions are distinguished that confer high, intermediate, or low activity (Table 1; Figure 2). Immunoblot data indicate that the variation in activity reflects differences in hybrid protein expression (Figures 4 and 5). Moreover, low-activity fusions that are not detected immunologically generally exhibit junctions in the cytoplasmic halves of putative transmembrane domains or in cytoplasmic loops. In contrast, high-activity fusions that are detected by immunoblots generally exhibit junctions in the periplasmic halves of putative transmembrane domains or in periplasmic loops. The data are consistent with previous studies (Gött & Boos, 1988; Calamia & Manoil, 1990; Lloyd & Kadner, 1990; Ujwal et al., 1995) indicating that fusions on the cytoplasmic surface are unstable and subjected to proteolysis. Conversely, degradation of chimeras that promote alkaline phosphatase export is partial, and a high- or intermediate-activity phenotype is observed (Figure 5). Finally, the alkaline phosphatase activity data presented here were not corrected for the rate of synthesis of the chimeras (Calamia & Manoil, 1990; Boyd et al., 1993). However, the variation in activity between high-activity fusions within individual clusters is in most instances less than 2-fold (Table 1), suggesting that correction for the rate of protein synthesis may not be necessary when clusters rather than isolated fusions are used to study topology.

Two aspects of the distribution of the low- and high-activity fusions are notable. First, high- and low-activity clusters alternate along the primary sequence of Mel permease (Figures 2 and 3). Second, high-activity clusters include residues located at or near every putative periplasmic loop, while residues located at or near every putative cytoplasmic loops are found in low-activity clusters. Taken together, the findings strongly support the contention that the hydrophilic domains in Mel permease are exposed alternately toward the periplasm or the cytoplasm in a pattern that is consistent with 12 membrane-spanning segments. Additional definition of the hydrophobic domains is obtained by examining the activity profile of the Mel−PhoA chimeras in light of the following: (a) the inner-half of out-going

domains is sufficient for alkaline phosphatase export; and (b) 11 residues of an in-coming transmembrane segment (i.e., the outer-half of the domain) are sufficient to prevent export of alkaline phosphatase to the periplasm (Calamia & Manoil, 1990). All out-going membrane-spanning domains except H7 fulfill the first postulate (Figure 3A). Regarding in-going segments, only H8, H12, and, to a lesser extent, H10 agree with the second. Therefore, the topology of the hydrophobic domains was readjusted by assuming that the transition from high to low activity occurs at the approximate middle of each transmembrane domain (Figure 3B).

The specific criteria used to readjust the topology of incoming membrane-spanning segments, namely, that the outer-half of the domain is sufficient to prevent export of alkaline phosphatase to the periplasm, deserves special comment. Results are presented showing that the alkaline phosphatase activity of fusions with junction points in two domains flanking a highly positively charged cytoplasmic loop is very low. Thus, the activity of six fusions (V50 toV66 in H2) just preceding the cytoplasmic C1 loop containing the R^+-S-R^+-W-G-K^+-S-K^+ sequence is as low as that of a fusion just following this stretch of residues (G83 in the inner-half of H3). Similarly, fusions T282 (this work) and P287 (Botfield et al., 1992) in the inner-half of H8 as well as fusions T297 and L305 fusions in the inner-half of H9, located upstream and dowstream from cytoplasmic loop C4 harboring the R^+-L-V-K^+-S-L-S-R^+-R^+ sequence display low activity. Previous studies of MalF protein suggest that a transmembrane (in-coming) segment sequence and the following cytoplasmic positively charged residues may be an absolute requirement to reduce alkaline phosphatase activity to low levels [Boyd and Beckwith (1989) and see review by Taxler et al. (1993)]. This conclusion does not satisfactorily account for the the low fusion activity level found in domains preceding the charged C1 and C4 loops of Mel permease. The results are more consistent with the hypothesis that an hydrophobic domain, probably limited to the outer-half of an in-coming membrane-spanning segment, may initiate the formation of a hairpin structure that reduces translocation of the PhoA moiety toward the periplasmic compartment. The inner-half domain of an in-coming segment, together with the positively charged cytoplasmic loop would further enhance the stability of the hairpin structure. Finally, by acting as a stop-transfer for insertion of the following out-going membrane segment, the positively charged cytoplasmic domain would partly specifies the position of the nascent segment residues that may be important for hydrophobic (or hydrophilic) interactions between the transmembrane domains on either side of the charged loop.

Several consequences of the revised secondary structure model presented in Figure 3 are noteworthy. It should first be mentioned that, although the topology of a number of loops was changed in order to comply with the placement of the activity transitions at the approximate middle of the membrane, the amino acid residues in the revised membrane-spanning segments still approximate the hydrophobic stretches predicted from the hydropathy plot. In addition, since the number of residues per helix is set at 21, when a given number of residues were moved from a periplasmic or cytoplasmic loop, an equivalent number were moved into or out of a corresponding loop. Most importantly, as a consequence of the manipulations, the central cytoplasmic loop of the permease is shortened by 14 residues and becomes comparable in size to a number of other loops (i.e., C2 and C5, Figure 3B).

According to the original secondary structure model of Mel permease (Botfeld et al., 1992; Pourcher et al., 1990), most of the charged residues in transmembrane domains are located in the N-terminal third of the protein in H1−H4. Among these charged residues, three Asp residues [D55 (H2), D59 (H2), and D124 (H4)] have been proposed to be involved in ion recognition, possibly by forming a coordination network for Na^+, Li^+, or H_3O^+ (Pourcher et al., 1993; Wilson & Wilson, 1994). Despite the changes suggested here for the H2 and H4 segments, the three Asp residues remain in hydrophobic domains. However, the revised model predicts that the three residues are closer to the cytoplasmic surface than suggested previously. In this context, D19, which was predicted to be in the N-terminal hydrophilic domain of Mel permease, is now placed at the cytoplasmic end of H1 at a depth comparable to D59 in H2 or D124 in H4. Interestingly, preliminary experiments (T. Pourcher and G. Leblanc, unpublished results) indicate that replacing D19 with Cys or Asn hampers the use of Na^+ (or Li^+) as a coupling ion in a manner reminiscent of mutant D59C, D59N, D124C, or D124N (Pourcher et al., 1993). Thus, D19 may also be part of the network of negatively charged residues that participate in ion recognition. Finally, D35, another acidic residue in H1, is closer to the periplasmic surface than to the cytoplasmic surface in the revised model. This may account for the minor role it appears to play in cation recognition (Pourcher et al., 1993a).

The revised Mel permease model predicts that several charged residues (R199, H202, and E203) are located in hydrophobic domain H6. The role of these residues in the mechanism of Mel permease remains to be elucidated. The charged residues in H6 may be involved in hydrogen bonding to α-D-galactopyranosides. Such interactions prevail in sugar binding to the periplasmic binding proteins of the bacterial ABC transport family [reviewed by Quiocho (1989)]. Alternatively, charged residues may have a structure/function role by interacting with an oppositely charged residues in a neighboring transmembrane domain. In plant light-harvesting complex LHC-II, the structure of which has been solved at 3.4 Å (Kuhlbrandt et al., 1994), two of the three transmembrane helices in the polypeptide are stabilized by salt bridges between Glu and Arg residues. In addition, the two ion-paired acidic residues are important for chlorophyll binding. With the lac permease of *E. coli*, charge-paired residues have been identified by using second-site suppressor analysis (King et al., 1991; Lee et al., 1993), site-directed mutagenesis (Sahin-Toth et al., 1992; Dunten et al., 1993; Sahin-Toth & Kaback, 1993), site-directed excimer fluorescence (Jung et al., 1993), and, most recently, by incorporating designed divalent metal binding sites (bis-His residues) into the protein (Jung et al., 1995; He et al., 1995a,b). The possibility that R199, H202, and/or E203 may be interacting with other charged residues in Mel permease is currently under investigation.

ACKNOWLEDGMENT

We thank Ms. Kerstin Stemple (Howard Hughes Medical Institute, UCLA) for synthesizing most of the oligonucleotides used in these studies. P. Lahitette (Laboratoire J.

Maetz/CEA) is acknowledged for excellent technical assistance.

REFERENCES

Botfield, M. C., & Wilson, T. H. (1989) *J. Biol. Chem. 264*, 11649−11652.

Botfield, M. C., Nuguchi, K., Tsuchiya, T., & Wilson, T. H. (1992) *J. Biol. Chem. 267*, 1818−1822.

Boyd, D., & Beckwith, J. (1989) *Proc. Natl. Acad. Sci. U.S.A., 86*, 9446−9450.

Boyd, D., Taxler, B., & Beckwith, J. (1993) *J. Bacteriol. 175*, 553−556.

Calamia, J., & Manoil, C. (1990) *Proc. Natl. Acad. Sci. U.S.A. 87*, 4937−4941.

Calamia, J., & Manoil, C. (1992) *J. Mol. Biol. 24*, 539−543.

Dunten, R. L., Sahin-Toth, M., & Kaback, H. R. (1993) *Biochemistry 32*, 3139−3145.

Gött, P., & Boos, W. (1988) *Mol. Microbiol. 2*, 655−663.

Hama, H., & Wilson, T. H. (1993) *J. Biol. Chem. 268*, 10060−10065.

He, M., Voss, J., Hubbell, W. L., & Kaback, H. R. (1995a) *Biochemistry 34*, 15661−15666.

He, M., Voss, J., Hubbell, W. L., & Kaback, H. R. (1995b) *Biochemistry 34*, 15667−15670.

Jung, K., Jung, H., Wu, J., Privé, G. G., & Kaback, H. R. (1993) *Biochemistry 32*, 12273−12278.

Jung, K., Voss, J., He, M., Hubbell, W. L., & Kaback, H. R. (1995) *Biochemistry 34*, 6272−6277.

Kaback, H. R. (1971) *Methods Enzymol. 25*, 698−709.

Kaback, H. R., Jung, K., Jung, H., Wu, J., Privé, G. G., & Zen, K. (1993) *J. Bioenerg. Biomembr. 25*, 627−636.

King, S. C., Hansen, C. L., & Wilson, T. H. (1991) *Biochem. Biophys. Acta 1062*, 177−186.

Kuhlbrandt, W., Wang, D. N., & Fujiyoshi, Y. (1994) *Nature (London) 367*, 614−621.

Laemmli, U. K. (1970) *Nature (London) 227*, 680−685.

Lee J., Hwang, P. P., & Wilson, T. H. (1993) *J. Biol. Chem. 268*, 20007−20015.

Lloyd, A. D., & Kadner, R. J. (1990) *J. Bacteriol. 172*, 1688−1693.

Lopilato, J., Tsuchiya, T., & Wilson, T. H. (1978) *J. Bacteriol. 134*, 147−156.

Lowry, O. H., Rosenbrough, N. J., Farr, A. L., & Randall, R. J. (1951) *J. Biol. Chem. 193*, 265−275.

Michaelis, S., Inouye, H., Oliver, D., & Beckwith, J. (1983) *J. Bacteriol. 154*, 366−374.

Manoil, C., & Beckwith, J. (1986) *Science 233*, 1403−1408.

Manoil, C., Mekalanos, J. J., & Beckwith, J. (1990) *J. Bacteriol. 172*, 515−518.

Pourcher, T., Bassilana, M., Sarkar, H. R., Kaback, H. R., & Leblanc, G. (1990a) *Philos. Trans. R. Soc. London, Ser. B 326*, 411−423.

Pourcher, T., Bassilana, M., Sarkar, H. K., Kaback, H. R., & Leblanc, G. (1990b) *Biochemistry 29*, 690- 696.

Pourcher, T., Sarkar, H. K., Bassilana, M., Kaback, H. R., & Leblanc, G. (1990c) *Proc. Natl. Acad. Sci. U.S.A. 87*, 468−472.

Pourcher, T., Deckert, M., Bassilana, M., & Leblanc, G. (1991) *Biochem. Biophys. Res. Commun. 178*, 1176−1181.

Pourcher, T., Bassilana, M., Sarkar, H. K., Kaback, H. R., & Leblanc, G. (1992) *Biochemistry 31*, 5225−5231.

Pourcher, T., Zani, M. L., & Leblanc, G. (1993) *J. Biol. Chem. 268*, 3209−3215.

Pourcher, T., Leclercq, S., Brandolin, G.. K.,& Leblanc, G. (1995) *Biochemistry* 34, 4412−4420.

Quiocho, F. A. (1990a) *Philos. Trans. R. Soc. London, Ser. B 326*, 341−351.

Sahin-Toth, M., & Kaback, H. R. (1993) *Biochemistry 32*, 10027−10035.

Sahin-Toth, M., Dunten, R. L., Gonzalez, A., & Kaback, H. R. (1992) *Proc. Natl. Acad. Sci. U.S.A. 89*, 10547−10551.

Traxler, B., Boyd, D., & Beckwith, J. (1993) *J. Membr. Biol. 132*, 1−11.

Ujwal, M. L., Jung, H., Bibi, E., Manoil, C., Altenbach, C., Hubbell, W. L., & Kaback, H. R. (1995) *Biochemistry 34*, 14909−14917.

von Heijne, G. (1992) *J. Mol. Biol.* 487−496.

Wilson, D. M., & Wilson, T. H. (1992) *J. Bacteriol. 174*, 3083−3086.

Wilson, D. M., & Wilson, T. H. (1994) *Biochem. Biophys. Acta 1190*, 225−230.

Yazyu, H., Shiota-Niiya, T., Shimamoto, T., Kanazawa, H., Futai, M., & Tsuchiya, T. (1984) *J. Biol. Chem. 259*, 4320−4326.

Yun, C.-H., Van Doren, S. R., Crofts, A. R., & Ginnis, R. B. (1991) *J. Biol. Chem. 266*, 10967−10973.

Zani, M. L., Pourcher, T., & Leblanc, G. (1993) *J. Biol. Chem. 268*, 3216−3221.

Zani, M. L., Pourcher, T., & Leblanc, G. (1994) *J. Biol. Chem. 269*, 24883−24889.

BI9527496